

Theory of morphotropic transformations in vanadium oxides

H. Katzke,^{1,*} P. Tolédano,^{1,2} and W. Depmeier¹

¹*Institute of Geosciences, Crystallography, University of Kiel, Olshausenstraße 40, 24098 Kiel, Germany*

²*Groupe "Structure des Matériaux Sous Conditions Extrêmes" SNBL/ESRF, Boîte Postale 220, 38043 Grenoble Cedex, France*

(Received 7 March 2003; published 31 July 2003)

A theory of the morphotropic transformations occurring between stoichiometric phases in the vanadium-oxide system is proposed. The interconnections between the different structures are shown to result from definite symmetry-breaking mechanisms from a common parent structure. The homologous series V_nO_{2n-1} and V_nO_{2n+1} are interpreted as sequences of lock-in commensurate phases. Identification of the order-parameter symmetries provides us with the form of the thermodynamic functions which allow for construction of the theoretical phase diagrams in which the different phases are inserted. The general procedure allowing for the description of morphotropic transformations is outlined.

DOI: 10.1103/PhysRevB.68.024109

PACS number(s): 64.70.Kb, 81.30.Kf

I. INTRODUCTION

A morphotropic transformation can be characterized^{1,2} as the structural change occurring between two adjacent homogeneous phases having different stoichiometries due to the variation in composition. Such transformations generally display a highly reconstructive mechanism and can be found in all multicomponent systems, the phase diagrams of which contain a series of stoichiometric phases separated by wide biphasic regions of coexistence, in which the content of neighboring phases varies continuously with concentration. Attempts have been made to describe theoretically ordered solid solutions by expressing their structures in terms of static concentration waves,³ combined with energy calculations based on the Ising model.⁴ However, to our knowledge, there exists no general theoretical framework that allows us to relate between them the entire set of stoichiometric phases for a given multicomponent system, including their mutual transformation mechanisms. In this work we show that a unifying description of the morphotropic transformations taking place in a given system can be performed by considering the symmetry-breaking mechanisms giving rise to the observed ordered structures. This description provides us with an insight into the structural mechanism underlying the transformations and allows us to construct the phase diagram in which the stoichiometric phases are inserted.

In Sec. II our approach is illustrated in the case of the vanadium-oxide system VO_x ($1 \leq x \leq 2.5$), the phase diagram of which contains not less than 16 homogeneous structures. We then discuss the general procedure which allows us to describe morphotropic transformations which is based on the Landau concepts and their extensions to incommensurate and reconstructive phase transitions (Sec. III).

II. THEORY OF THE VO_x PHASE DIAGRAM

A. The Magnéli phases

Figure 1 reproduces the experimental phase diagram of the V-O system. Its central part (V_2O_3 - VO_2) contains seven homogeneous phases: VO_2 , V_2O_3 and the five intermediate Magnéli phases⁵ corresponding to the homologous series V_nO_{2n-1} with $3 \leq n \leq 7$. Let us first describe the connections

between the rutile-type structure, denoted by $VO_2(R)$, of VO_2 and the structure of the Magnéli phases in which we include the V_8O_{15} and V_9O_{17} compositions.^{6,7} Table I gives the relationship between the basic vectors \mathbf{t}_1 , \mathbf{t}_2 , and \mathbf{t}_3 of the triclinic unit cells of the V_nO_{2n-1} structures and the basic vectors \mathbf{a} , \mathbf{b} , and \mathbf{c} of the tetragonal unit cell of $VO_2(R)$, according to the description given by Katzke and Schlögl.⁸ One can see that for $4 \leq n \leq 9$, one has

$$\mathbf{t}_1 = \mathbf{a} - \mathbf{c}, \quad \mathbf{t}_2 = \mathbf{b} - \mathbf{a} - \mathbf{c}, \quad \mathbf{t}_3 = \frac{1}{2}(2n-1)(\mathbf{b} - \mathbf{c}), \quad (1)$$

whereas for $n = 3$, the \mathbf{t}_1 translation is doubled. Therefore, if V is the unit-cell volume of $VO_2(R)$, the unit cell of the n th member of the homologous series is $[(2n-1)/2]V$ for $4 \leq n \leq 9$ and $(2n-1)V$ for $n = 3$, as indicated in column 3 of Table I. Column 4 of the table lists the Wyckoff positions occupied by the atoms in each structure.

From Eq. (1), one can deduce the critical wave vectors \mathbf{k}_n of the primitive tetragonal Brillouin zone associated with the transformations from $VO_2(R)$ to the V_nO_{2n-1} structures. For $4 \leq n \leq 9$ one finds $\mathbf{k}_n = [4/(2n-1)]\mathbf{k}_1$ with $\mathbf{k}_1 = (\pi/\mathbf{a}, 2\pi/\mathbf{a}, \pi/\mathbf{c})$, while for $n = 3$, $\mathbf{k}_3 = \frac{4}{5}\mathbf{k}_2$ with $\mathbf{k}_2 = (\pi/\mathbf{a}, \pi/2\mathbf{a}, \pi/\mathbf{c})$. Accordingly, as summarized in Fig. 2(a), the Magnéli phases can be interpreted as a sequence of low-symmetry structures, induced from the parent $VO_2(R)$ structure by successive first-order lock-in transitions with the fractional lock-in vectors $\frac{4}{17}\mathbf{k}_1$ (V_9O_{17}), $\frac{4}{15}\mathbf{k}_1$ (V_8O_{15}), $\frac{4}{13}\mathbf{k}_1$ (V_7O_{13}), $\frac{4}{11}\mathbf{k}_1$ (V_6O_{11}), $\frac{4}{9}\mathbf{k}_1$ (V_5O_9), $\frac{4}{7}\mathbf{k}_1$ (V_4O_7), and $\frac{4}{5}\mathbf{k}_2$ (V_3O_5). This is consistent with the description given by Hirotsu *et al.*⁹ of the Magnéli phases in terms of long period modulated structures, where one oxygen layer is removed at every n^{th} V layer in the direction perpendicular to the (211) plane of $VO_2(R)$. As n becomes large the difference in the thermodynamic stability among the phases with closer n becomes small, creating the condition for a "microsyntactic" intergrowth,¹⁰ meaning that two neighboring structures intergrow in narrow bands, down to a few unit cells, with a mixing of their periods, and the lock-in structures result from an accumulation of lattice defects.

Since the \mathbf{k}_n and \mathbf{k}_3 critical wave vectors are located in general positions inside the tetragonal Brillouin zone, the irreducible representations (IR's) inducing the $P4_2/mnm \rightarrow$

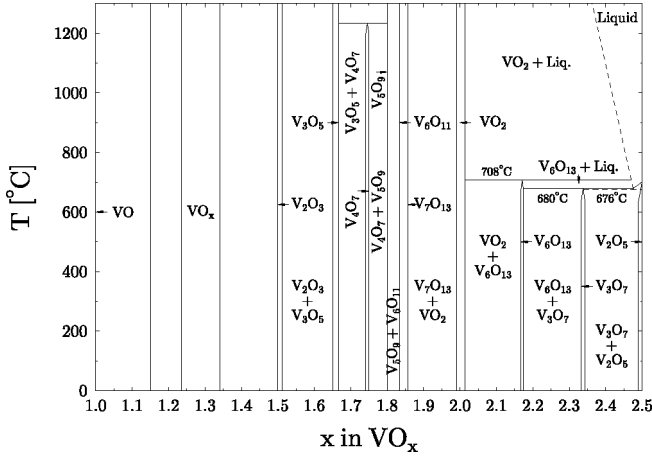


FIG. 1. Experimental phase diagram of the VO_x system ($1 \leq x \leq 2.5$) from Refs. 17,18, and 30.

$P\bar{1}$ symmetry changes are 16 dimensional. This dimension is determined by the number of branches of the stars k_n^* and k_3^* (16) and by the order (1) of the invariance group of one branch, which is C_1 . A Landau symmetry analysis shows that the triclinic symmetry is obtained for the equilibrium values $\eta = \eta_1 = \eta_2 \neq 0, \eta_3 = \dots = \eta_{16} = 0$ of the corresponding order-parameter components, where η_1 and η_2 express the ordering plus shifting mechanisms,⁸ transforming the VO_2 structure into the structure of the Magnéli phases. The order-parameter expansion contains even degree invariants truncated at the degree $2m$ with $m \geq 3$ and one odd-degree invariant of power $2n - 1$ with $4 \leq n \leq 9$. Consequently, the effective order-parameter expansion associated with the $\text{VO}_2(R) \rightarrow \text{V}_n\text{O}_{2n-1}$ transformation reads

$$F(T, x, \eta) = F_0(T, x) + \frac{a_1}{2} \eta^2 + \frac{a_2}{4} \eta^4 + \dots + \frac{a_{2m}}{2m} \eta^{2m} + \frac{\delta_n}{2n-1} \eta^{2n-1}, \quad (2)$$

where the odd δ_n invariants play the role of the lock-in terms favoring the transformation to the lock-in commensurate structures.¹¹ Figure 2(b) shows the theoretical phase diagram in the (a_1, δ_n) plane, as deduced from the minimization of F with respect to η , when assuming that a_1 depends linearly on temperature T and concentration x , whereas δ_n is linearly dependent on the x variable. Although the sequential order of the Magnéli phases is verified in this phase diagram, the property that $\text{VO}_2(R)$ merges at a triple point with all pairs of neighboring Magnéli phases is inconsistent with the topology of the experimental phase diagram of Fig. 1. It suggests that a higher-symmetry parent structure, from which $\text{VO}_2(R)$ derives, has to be considered, with $\text{VO}_2(R)$ representing the limit lock-in structure for large n in the $\text{V}_n\text{O}_{2n-1}$ series.

In the rutile-type structure of $\text{VO}_2(R)$, as well as in the homologous series $\text{V}_n\text{O}_{2n-1}$, the oxygen atoms form a distorted hexagonal-close-packed array,^{12,13} whereas in the corundum-type structure of V_2O_3 , they form an almost ideal hexagonal close packing.¹⁴ It yields to take as a parent structure for $\text{VO}_2(R)$ and V_2O_3 their *maximal common substructure* which, as shown in Fig. 3(a), consists of a bilayer (AB) hexagonal-close-packing structure. In this bilayer structure of symmetry $P6_3/mcm$, denoted hereafter as the L structure, the V atoms are disordered over six ($2b$) and ($4d$) positions. The formation of the bilayer $\text{VO}_2(R)$ structure from the L structure results from a fractional occupancy $x = \frac{1}{2}$ of three V atoms over the six preceding positions, whereas the six-

TABLE I. Crystallographic features of the V-O compounds described in the present work.

Oxide	Basic lattice vectors	Unit cell volume	Wyckoff positions	Reference
$\text{VO}_2(R)$	$\mathbf{a}, \mathbf{b}, \mathbf{c}$	V	$V(2a), O(4f)$	12
V_9O_{17}	$t_1 = \mathbf{a} - \mathbf{c}, t_2 = \mathbf{b} - \mathbf{a} - \mathbf{c}, t_3 = \frac{17}{2}(\mathbf{b} - \mathbf{c})$	$\frac{17}{2}V$	$V1-V8(2i), V9(1b), V10(1g), O1-O17(2i)$	7
V_8O_{15}	$t_1 = \mathbf{a} - \mathbf{c}, t_2 = \mathbf{b} - \mathbf{a} - \mathbf{c}, t_3 = \frac{15}{2}(\mathbf{b} - \mathbf{c})$	$\frac{15}{2}V$	$V1-V8(2i), O1-O15(2i)$	6
V_7O_{13}	$t_1 = \mathbf{a} - \mathbf{c}, t_2 = \mathbf{b} - \mathbf{a} - \mathbf{c}, t_3 = \frac{13}{2}(\mathbf{b} - \mathbf{c})$	$\frac{13}{2}V$	$V1-V6(2i), V7(1b), V8(1g), O1-O13(2i)$	13
V_6O_{11}	$t_1 = \mathbf{a} - \mathbf{c}, t_2 = \mathbf{b} - \mathbf{a} - \mathbf{c}, t_3 = \frac{11}{2}(\mathbf{b} - \mathbf{c})$	$\frac{11}{2}V$	$V1-V6(2i), O1-O11(2i)$	13
V_5O_9	$t_1 = \mathbf{a} - \mathbf{c}, t_2 = \mathbf{b} - \mathbf{a} - \mathbf{c}, t_3 = \frac{9}{2}(\mathbf{b} - \mathbf{c})$	$\frac{9}{2}V$	$V1-V4(2i), V5(1b), V6(1g), O1-O9(2i)$	27
V_4O_7	$t_1 = \mathbf{a} - \mathbf{c}, t_2 = \mathbf{b} - \mathbf{a} - \mathbf{c}, t_3 = \frac{7}{2}(\mathbf{b} - \mathbf{c})$	$\frac{7}{2}V$	$V1-V4(2i), O1-O7(2i)$	28
V_3O_5	$t_1 = 2(\mathbf{a} - \mathbf{c}), t_2 = \mathbf{b} - \mathbf{a} - \mathbf{c}, t_3 = \frac{5}{2}(\mathbf{b} - \mathbf{c})$	$5V$	$V1-V4(2i), V5(1b), V6(1f), V7(1g), V8(1h), O1-O10(2i)$	29
L	$\mathbf{a}_L, \mathbf{b}_L, \mathbf{c}_L$	V_L	$V1(2b), V2(4d), O(6g)$	
$\text{VO}_2(R)$	$\mathbf{b}_L, \mathbf{c}_L, \frac{1}{3}(2\mathbf{a}_L + \mathbf{b}_L)$	$\frac{2}{3}V_L$	$V(2a), O(4f)$	12
V_2O_3	$\mathbf{a}_L, \mathbf{b}_L, 3\mathbf{c}_L$	$3V_L$	$V(12c), O(18e)$	14
VO_x	$\mathbf{a}_c, \mathbf{b}_c, \mathbf{c}_c$	V_c	$V(4a), O(4b)$	17
$0.87 \leq x \leq 1.11$				
$\text{VO}_{1.24}$	$2(\mathbf{a}_c + \mathbf{b}_c), 2(\mathbf{b}_c - \mathbf{a}_c), 2\mathbf{c}_c$	$16V_c$	$V1(4a), V2-V3(16f), V4(16g), V5(16h), O1-O2(16h), O3(32i)$	18
V_2O_5	$3\mathbf{a}_c, \mathbf{b}_c, \mathbf{c}_c$	$3V_c$	$V1(4f), O1-O2(4f), O3(2a)$	21
V_3O_7	$6\mathbf{a}_c, \mathbf{b}_c, 5\mathbf{c}_c$	$30V_c$	$V1(4e), V2-V5(8f), O1(4e), O2-O11(8f)$	23
V_6O_{13}	$3\mathbf{a}_c, \mathbf{b}_c, 3\mathbf{c}_c$	$9V_c$	$V1-V3(4i), O1-O6(4i), O7(2b)$	22
$\text{VO}_2(B)$	$3\mathbf{a}_c, \mathbf{b}_c, 2\mathbf{c}_c$	$6V_c$	$V1-V2(4i), O1-O4(4i)$	19

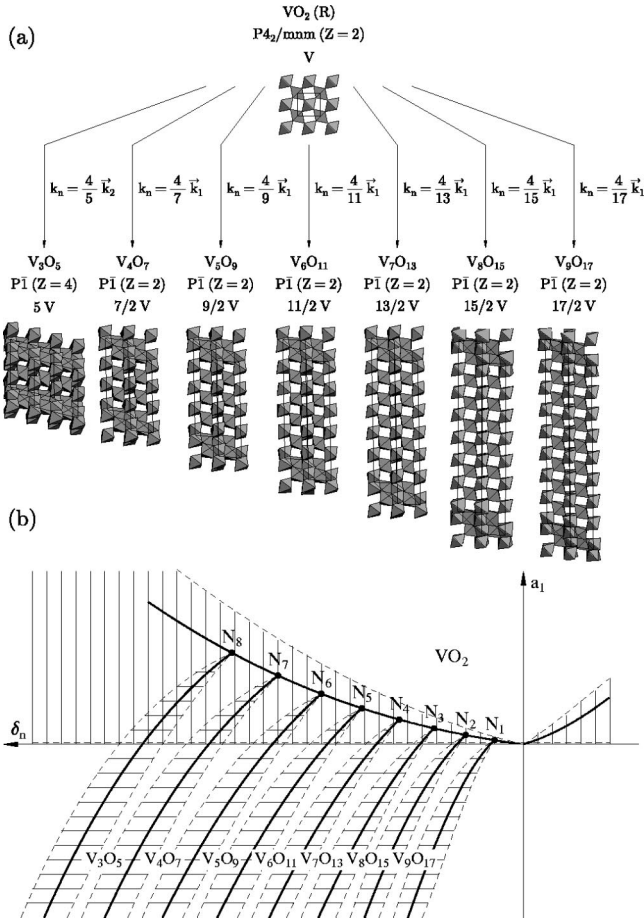


FIG. 2. (a) Structural connections between the Magnéli phases and the $VO_2(R)$ phase. (b) Theoretical phase diagram associated with the free energy defined by Eq. (2).

layered V_2O_3 close-packed structure is obtained for an occupancy $x = \frac{2}{3}$ of four V atoms. Figure 3(b) summarizes the $L \rightarrow VO_2(R)$ and $L \rightarrow V_2O_3$ transformation mechanisms. One can see that both mechanisms are associated with a breaking of the hexagonal translational symmetry, with a doubling of the lattice parameter in the $[100]$ hexagonal direction for $VO_2(R)$, and a tripling of the c -hexagonal lattice parameter for V_2O_3 . A ferroelastic monoclinic deformation, involving the spontaneous strain components ($e_{xx} - e_{yy}$) and e_{xy} is also required for the formation of $VO_2(R)$, whereas a ferroelastic¹⁵ rhombohedral deformation of the L structure is necessary for obtaining V_2O_3 . Atomic shifts bring the V and O atoms in their specific rutile-type and corundum-type positions.

Figure 3(b) indicates the critical wave vectors and order-parameter symmetries involved in the formation of $VO_2(R)$ and V_2O_3 . Taking into account only the primary translational symmetry-breaking order parameters,¹⁶ respectively, denoted as ζ and ξ , yields the Landau free energy:

$$F(T, x, \zeta, \xi) = F_0(T, x) + \frac{\alpha_1}{2} \zeta^2 + \frac{\beta_1}{4} \zeta^4 + \frac{\gamma_1}{6} \zeta^6 + \frac{\alpha_2}{2} \xi^2 + \frac{\beta_2}{4} \xi^4 + \frac{\gamma_2}{6} \xi^6 + \frac{\delta}{2} \zeta^2 \xi^2. \quad (3)$$

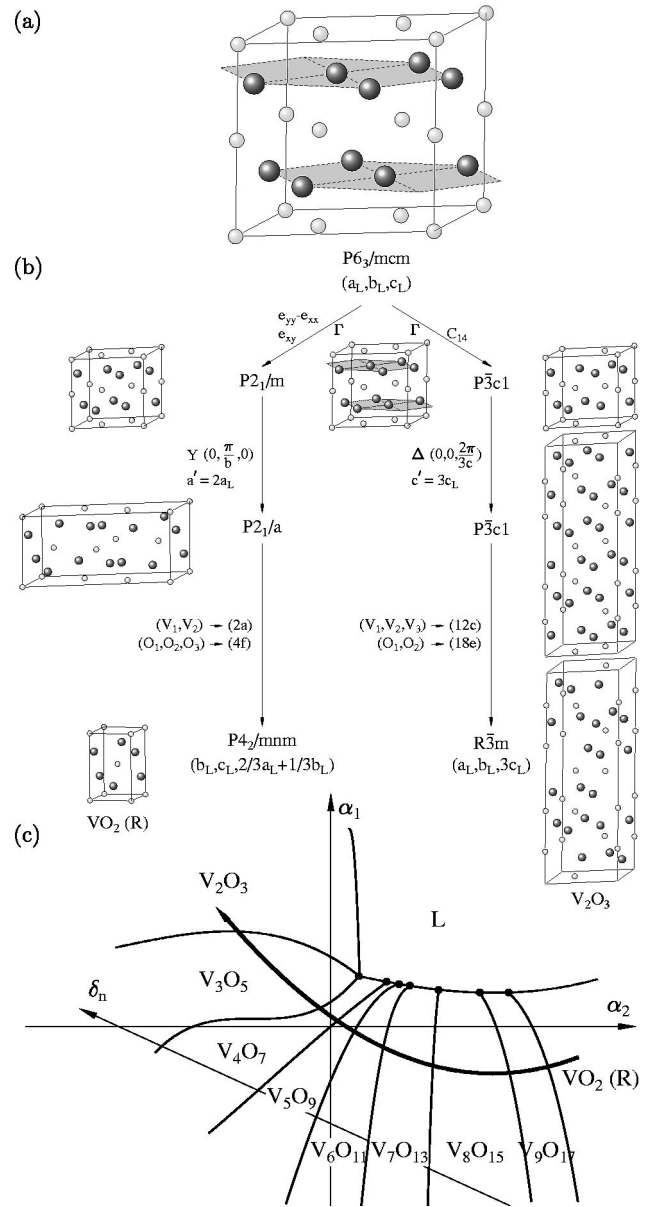


FIG. 3. (a) Maximal common substructure of $VO_2(R)$ and V_2O_3 (L structure). (b) Symmetry breaking mechanisms leading to the $VO_2(R)$ and V_2O_3 structures from the L structure. (c) Theoretical phase diagram corresponding to the free energy expressed by Eq. (3). Vanadium atoms are represented by smaller gray circles and oxygen atoms by larger black circles. Comments on the figures are given in the text.

Figure 3(c) shows the phase diagram associated with F in the (α_1, α_2) plane, obtained by a minimization of F with respect to ζ and ξ and assuming $\delta > 0$, $\beta_1 < 0$, $\beta_2 < 0$, and $\beta_1 \beta_2 - \delta^2 > 0$. In addition to the $VO_2(R)$ ($\zeta \neq 0, \xi = 0$) and V_2O_3 ($\zeta = 0, \xi \neq 0$) phases, an intermediate phase is stabilized for $\zeta \neq 0, \xi \neq 0$, which possesses the triclinic $P\bar{1}$ symmetry of the Magnéli phases.

B. The V_nO_{2n+1} series

The preceding description concerns the structures which have been disclosed between VO_2 and V_2O_3 , i.e., corre-

sponding to $2 \geq x \geq 1.5$ in VO_x . For $x < 1.5$ two additional structures have been identified: a face-centered-cubic structure¹⁷ ($Fm\bar{3}m$, $Z=4$) for $1.00 \leq x \leq 1.17$ and a tetragonal structure¹⁸ ($I4_1/amd$, $Z=1$) for $1.24 \leq x \leq 1.33$. In both structures, shown in Fig. 4(a), the oxygen atoms are cubic-close-packed and the cubic-to-tetragonal transformation mechanism corresponds to an ordering of the vanadium atoms from $4(a)$ fcc positions to the interstitial positions $16(h)$, $16(f)$, and $16(g)$ as indicated in Table I. The relationship between the basic vectors of the tetragonal ($\mathbf{a}_t, \mathbf{b}_t, \mathbf{c}_t$) and cubic ($\mathbf{a}_c, \mathbf{b}_c, \mathbf{c}_c$) unit cells is

$$\mathbf{a}_t = 2(\mathbf{a}_c + \mathbf{b}_c), \quad \mathbf{b}_t = 2(\mathbf{b}_c - \mathbf{a}_c), \quad \mathbf{c}_t = 2\mathbf{c}_c. \quad (4)$$

It corresponds to the critical wave vector $\mathbf{k} = (0, \pi/a, \pi/a)$ located inside the fcc Brillouin zone. One can verify that the $I4_1/amd$ space-group symmetry with a 32-fold multiplication of the $Fm\bar{3}m$ primitive cell is induced by a 12-dimensional IR of the $Fm\bar{3}m$ group.

The fcc structure of VO_x ($x \cong 1$) can be used as a parent structure for the $\text{V}_n\text{O}_{2n+1}$ structures, with $n = 2, 3, 6$, located on the right-hand side of the phase diagram of Fig. 1, and of the metastable $\text{VO}_2(B)$ (Ref. 19) form of VO_2 , obtained by reduction of V_2O_5 . Following the suggestion given by Hyde and Andersson,²⁰ V_2O_5 , V_3O_7 , V_6O_{13} , and $\text{VO}_2(B)$ can be considered as oxygen deficient fcc structures, which are deduced from the cubic structure by introducing different ordered vacancies in the oxygen close-packing array. The atomic positions in each $\text{V}_n\text{O}_{2n+1}$ phase are given in Table I. If x_V and x_O are the respective concentrations of vanadium and oxygen, the threefold orthorhombic structure ($Pm\bar{m}n, Z=2$) of V_2O_5 (Ref. 21) corresponds to $x_V = \frac{1}{3}$, $x_O = \frac{5}{6}$, the ninefold V_6O_{13} structure ($C2/m, Z=2$) (Ref. 22) is obtained for $x_V = \frac{1}{3}$, $x_O = \frac{13}{18}$, and the 30-fold idiosyncratic structure of V_3O_7 ($C2/c, Z=12$) (Ref. 23) is stabilized for $x_V = 0.3$, $x_O = 0.7$. In the sixfold monoclinic structure of $\text{VO}_2(B)$ ($C2/m, Z=8$) (Ref. 19), $x_V = \frac{1}{3}$ and $x_O = \frac{2}{3}$. Figure 4(b) represents the structures of the homologous series $\text{V}_n\text{O}_{2n+1}$ for $n = 2, 3, 6$, the structure of $\text{VO}_2(B)$, and the connections with the fcc structure of VO. It has to be noted that the monoclinic V_6O_{13} and $\text{VO}_2(B)$ structures involve a collapse of the fcc layers along the \mathbf{c} cubic axis, since the ordering mechanism leaves one out of six layers filled by vacancies in V_6O_{13} and one out of four vacant fcc layers in $\text{VO}_2(B)$. This collapsing induces the observed monoclinic shear deformation.

The breaking of translational symmetry with respect to the fcc structure corresponds for V_2O_5 , V_6O_{13} , and $\text{VO}_2(B)$ to critical wave vectors located in the same direction $\mathbf{k} = (2\pi/3a, 0, \mathbf{k}_z)$ inside the fcc Brillouin zone, with $\mathbf{k}_z = 0$, $\mathbf{k}_z = 2\pi/3a$, and $\mathbf{k}_z = \pi/a$. For V_3O_7 the critical wave-vector is $\mathbf{k} = (2\pi/6a, 0, 2\pi/5a)$. Accordingly, a lock-in mechanism, analogous to the one proposed for the $\text{V}_n\text{O}_{2n-1}$ series, can be assumed for the $\text{V}_n\text{O}_{2n+1}$ series, $\text{VO}_2(B)$ playing the role of the limit lock-in structure. The onset of the $\text{V}_n\text{O}_{2n+1}$ lock-in phases can be related to the successive fractional concentrations of vacancies in the oxygen packing: (1

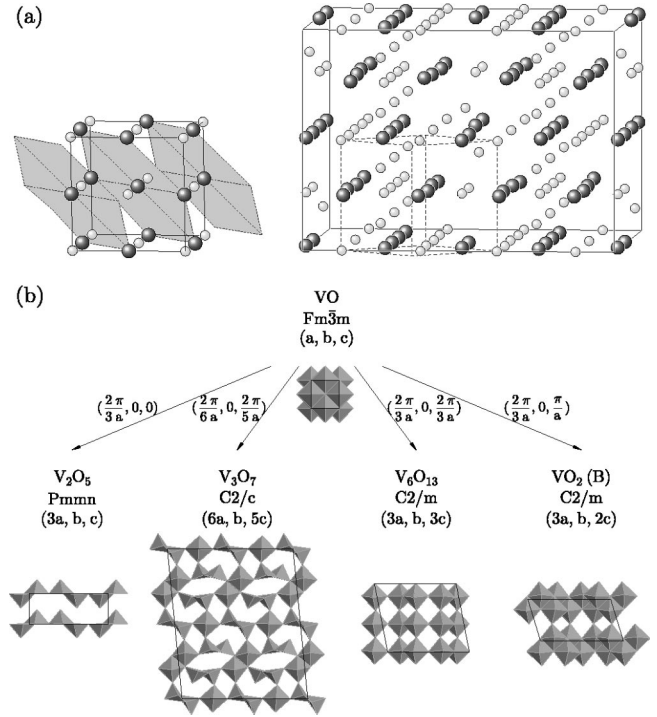


FIG. 4. (a) Face-centered-cubic structure of VO and the tetragonal structure of VO_x ($1.24 \leq x \leq 1.33$). (b) Symmetry-breaking mechanisms leading to the structures of the $\text{V}_n\text{O}_{2n+1}$ series ($n = 2, 3, 6$) and $\text{VO}_2(B)$ from the cubic VO structure. Vanadium atoms are represented by smaller gray circles and oxygen atoms by larger black circles.

$-x_O) = \frac{1}{6}$ (V_2O_5), $\frac{5}{18}$ (V_6O_{13}), 0.3 (V_3O_7), and $\frac{1}{3}$ ($\text{VO}_2(B)$). Figure 5(a) shows the linear dependence of $(1 - x_O)$ in the function of the V valence, which is well verified except for V_3O_7 . A determination of the still unknown structure of V_4O_9 ,²⁴ for which a V_2O_5 related structural model with ordered oxygen vacancies and orthorhombic symmetry has been proposed,²⁵ should provide a further test for the lock-in nature of the $\text{V}_n\text{O}_{2n+1}$ phases.

Denoting $\eta_1 = \rho \cos \Theta$ and $\eta_2 = \rho \sin \Theta$ the nonzero equilibrium values of the order-parameter components associated with the fcc $\rightarrow [\text{V}_n\text{O}_{2n+1}$ or $\text{VO}_2(B)]$ transition,²⁶ one gets the effective Landau free energy

$$F(T, x, \rho, \Theta) = F_0(T, x) + \frac{a_1}{2} \rho^2 + \dots + \frac{a_m \rho^{2m}}{2m} + \frac{\delta_P}{P} \rho^P \cos P \Theta, \quad (5)$$

where the δ_P invariants (with $P \geq 3$) play the role of the lock-in terms. Figure 5(b) shows the phase diagram resulting from the minimization of F with respect to ρ and Θ in the (a_1, δ_P) plane. It displays the V_2O_5 - V_6O_{13} - $\text{VO}_2(B)$ phase sequence with the same sequential order as in Fig. 1.

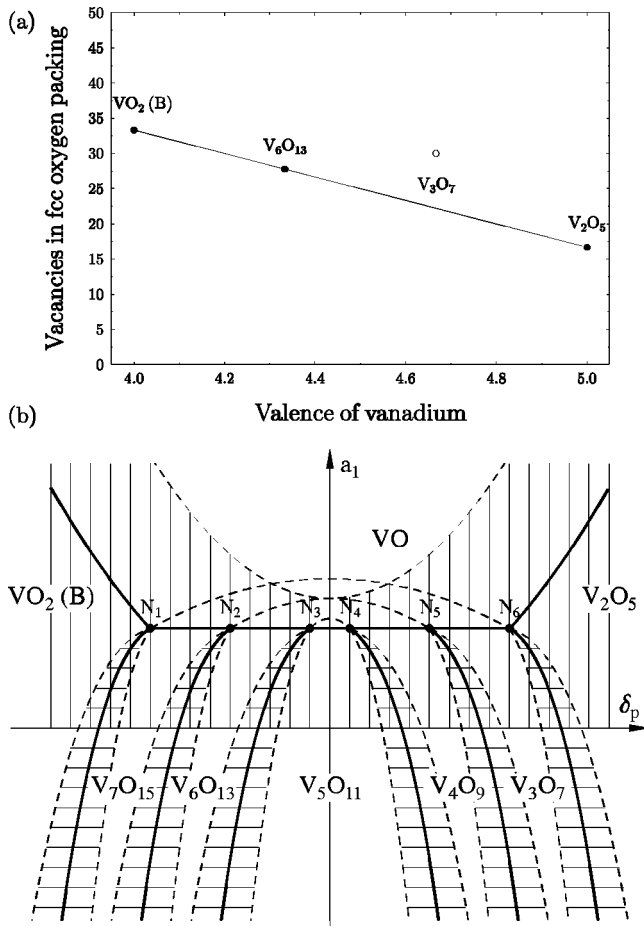


FIG. 5. (a) Dependence of the fractional concentrations of vacancies in the oxygen packing as a function of the V valence. (b) Corresponding theoretical phase diagram which includes the V₇O₁₅, V₅O₁₁, and V₄O₉ phases predicted theoretically.

C. The parent structure in the V-O system

The fcc parent structure assumed for the V_nO_{2n+1} series and VO₂(B) corresponds to three stacked hexagonal-(ABC) close-packed layers. It therefore has a simple relationship with the (AB) bilayer L structure used as the parent structure for the V_nO_{2n-1} series and VO₂(R). Figure 6 shows that the maximal substructure common to the fcc and L structures is composed by a monolayer structure of symmetry $P6/mmm$, in which the atoms are randomly distributed over the V positions 1(a) and 2(c) and O positions 1(b) and 2(d). The stacking of such hexagonal monolayers in which one over three positions are randomly occupied constitutes a *statistically disordered polytype structure*, from which the L and fcc structures can be deduced by the following ordering mechanisms, represented in Fig. 6 : (1) The $P6/mmm$ ($Z=1$) $\rightarrow P6_3/mcm$ ($Z=6$) bilayer ordering yields the V atoms at positions 2(b) and 4(a), whereas the O atoms are at position 6(g). The corresponding sixfold multiplication of the unit cell is induced by a two-dimensional IR at the H point [$\mathbf{k}=(4\pi/3a, 0, \pi/c)$] of the hexagonal Brillouin zone. (2) The $P6/mmm \rightarrow Fm\bar{3}m$ cell-quadrupling mechanism yields an occupancy of V and O atoms, respectively at the positions

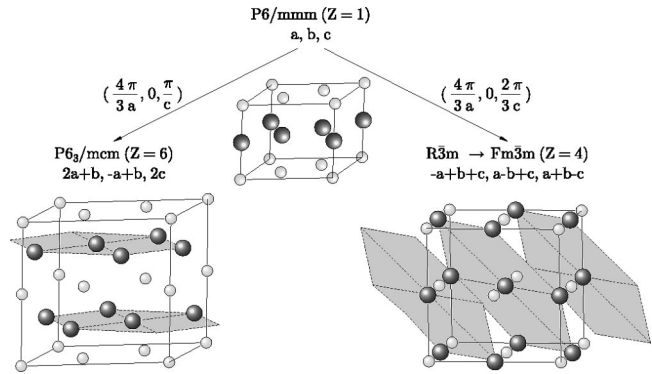


FIG. 6. Connections between the VO and L structures with the parent disordered polytype unit cell structure. Vanadium atoms are represented by smaller gray circles and oxygen atoms by larger black circles.

4(a) and 4(b). It is associated with a four-dimensional IR at [$\mathbf{k}=(4\pi/3a, 0, 2\pi/3c)$] which gives rise to the rhombohedral symmetry $R\bar{3}m$, identifying to the fcc rhombohedron when the angles between the lattice vectors are 60° .

The existence of a parent disordered polytype structure, assumed in our approach, for all the structures found in the V-O system has a number of implications. In particular, these structures should be *intrinsically faulted*. There are two different origins for the stacking faults : (1) one type of stacking faults is symmetry induced and independent of the temperature. It results from the existence of antiphase domains (deformation stacking faults³¹) which occur at the monolayer (hexagonal polytype) \rightarrow bilayer (L structure) transition as well as in the disordered polytype \rightarrow fcc transition. This latter transition should also produce orientational domains (twinning stacking faults³¹) transforming into one another by the lost sixfold rotations. (2) Another type of temperature-dependent defects originates in the ordering mechanism assumed for the formation of structures derived from the L and fcc structures. In the disordered polytype phase each close-packed layer corresponds to a stacking fault. The ordering process can be characterized by the number $\Delta=1-(N_d/N)$, where N is the total number of layers and N_d is the number of stacking faults. One has $\Delta=0$ in the disordered polytype parent structure and $\Delta=1$ in an ideal ordered structure. Intermediate states correspond to $0 < \Delta < 1$. The value of Δ at a given temperature and pressure is determined by the number of defects. In the ordered structures the asymptotic value of Δ will reflect the symmetry-induced type of stacking faults, whereas in the disordered structures Δ accounts as well for the temperature-dependent defects.

From the preceding consideration one can infer a qualitative picture for the segregation process leading to the formation of the ordered V-O structures, inspiring ourselves from the ordering mechanism recently proposed for the close-packed structures of cobalt³⁴. Below the melt, the structures are partially ordered ($0 < \Delta < 1$) and formed by ordered regions surrounded by disordered sequences of close-packed polytypes. On cooling, the fraction of disordered sequences of layers reduce and the intrinsically faulted ordered regions tend to coalesce. This picture provides a justification and an

interpretation of the hexagonal disordered polytype structure which has been assumed from symmetry considerations to be the parent structure in the V-O system.

III. SUMMARY AND DISCUSSION

In summary, a phenomenological approach has been proposed for describing the transformation mechanisms associated with the stoichiometric phases found in the vanadium-oxide system. The homologous series V_nO_{2n-1} and V_nO_{2n+1} structures have been interpreted as sequences of lock-in phases, the $VO_2(R)$ and $VO_2(B)$ being the limit lock-in structures for the two series. The interconnections between the different structures have been shown to result from definite symmetry-breaking mechanisms from a common parent structure. Identification of the corresponding order-parameter symmetries has allowed for construction the thermodynamic potentials associated with the different classes of structures involved in the experimental phase diagram, and to deduce the partial theoretical phase diagram for each structural class. Our proposed approach differs essentially from the concentration-wave approach³ used for describing the homogeneous structures of solid solutions. In this respect, the theoretical model of the Magnéli phases proposed by Pokrovskii and Khachatryan⁴ assumes a common

bcc matrix for the different structures, whereas we have shown that all the vanadium-oxide phases can be ultimately derived from a common disordered polytype hexagonal structure.

The procedure implicitly followed for obtaining a unified description of the structural mechanisms occurring in the V-O system comprises in (1) separating in the phase diagram of this system the different set of phases which are structurally interconnected, and (2) finding a common parent structure for each set of phases and ultimately a common parent structure for the full set of structures. For each of the preceding steps a (Landau) symmetry analysis was performed which yielded the relevant order-parameter symmetries associated with the transitions from the parent-to-the daughter phases. It revealed that the stoichiometric phases can be considered as *limit states*, which are obtained for specific (critical) displacements or probabilities of occupancy of the atoms in given sites. This situation is reminiscent of reconstructive phase transitions,³² and shows that morphotropic transitions can be treated into the same theoretical framework that was recently proposed for transitions of the reconstructive type.^{33,34}

ACKNOWLEDGMENT

This work has been supported by the German Science Foundation.

*Email address: hanne@min.uni-kiel.de

¹L. Bragg and F. Claringbull, *Crystal Structure of Minerals* (Bell, London, 1965).

²J.-C. Tolédano, R.S. Berry, P.J. Brown, A.M. Glazer, R. Metseelaar, D. Pandey, J.M. Perez-Mato, R.S. Roth, and S.C. Abrahams, *Acta Crystallogr., Sect. A: Found. Crystallogr.* **57**, 614 (2001).

³A.G. Khachatryan, *Prog. Mater. Sci.* **22**, 1 (1978).

⁴B.I. Pokrovskii and A.G. Khachatryan, *J. Solid State Chem.* **61**, 137 (1986); **61**, 154 (1986).

⁵A. Magnéli, *Acta Crystallogr.* **6**, 495 (1953).

⁶S. Andersson and L. Jahnberg, *Ark. Kemi* **21**, 413 (1964).

⁷H. Sato, N. Otsuka, H. Kuwamoto, and G.L. Liedl, *J. Solid State Chem.* **44**, 212 (1982).

⁸H. Katzke and R. Schlögl, *Z. Kristallogr.* **218**, 432 (2003).

⁹Y. Hirotsu and H. Sato, *Mater. Res. Bull.* **15**, 41 (1980).

¹⁰Y. Hirotsu, Y. Tsunashima, S. Nagakura, H. Kuwamoto, and H. Sato, *J. Solid State Chem.* **43**, 33 (1982).

¹¹J.C. Tolédano and P. Tolédano, *The Landau Theory of Phase Transitions* (World Scientific, Singapore, 1987), Chap. 5.

¹²D.B. McWhan, M. Marezio, J.P. Remeika, and P.D. Dernier, *Phys. Rev. B* **10**, 490 (1974).

¹³H. Horiuchi, N. Morimoto, and M. Tokonami, *J. Solid State Chem.* **17**, 407 (1976).

¹⁴C.E. Rice and W.R. Robinson, *J. Solid State Chem.* **21**, 145 (1977).

¹⁵P. Tolédano and J.C. Tolédano, *Phys. Rev. B* **16**, 386 (1977).

¹⁶The tetragonal and rhombohedral deformations of the hexagonal structure are small and can be assumed to be secondary order parameters although they are symmetry-breaking quantities.

¹⁷R.E. Loehman, C.N. Ramachandra Rao, and J.M. Honig, *J. Phys. Chem.* **73**, 1781 (1969).

¹⁸M. Morinaga and J.B. Cohen, *Acta Crystallogr., Sect. A: Cryst. Phys., Diffr., Theor. Gen. Crystallogr.* **35**, 745 (1979).

¹⁹F. Théobald, R. Cabala, and J. Bernard, *J. Solid State Chem.* **17**, 431 (1976).

²⁰B.G. Hyde and S. Andersson, *Inorganic Crystal Structures* (Wiley, New York, 1989).

²¹R. Enjalbert and J. Galy, *Acta Crystallogr., Sect. C: Cryst. Struct. Commun.* **42**, 1467 (1986).

²²O. Bergstroem, T. Gustafsson, and J.O. Thomas, *Solid State Ionics* **110**, 179 (1998).

²³K. Waltersson, B. Forslund, K.-A. Wilhelmli, S. Andersson, and J. Galy, *Acta Crystallogr., Sect. B: Struct. Crystallogr. Cryst. Chem.* **30**, 2644 (1974).

²⁴F. Théobald, R. Cabala, and J. Bernard, *C. R. Seances Acad. Sci., Ser. C* **269**, 1209 (1969).

²⁵G. Grymonprez, L. Fiermans, and J. Vennik, *Acta Crystallogr., Sect. A: Cryst. Phys., Diffr., Theor. Gen. Crystallogr.* **33**, 834 (1977).

²⁶The IR's of the $Fm\bar{3}m$ space group inducing the V_nO_{2n+1} structures possess, respectively, $6(V_2O_5)$, $12(V_6O_{13})$, and $24[V_3O_7, VO_2(B)]$ dimensions, but only two components of the corresponding order parameters ($\eta_1 \neq \eta_2$) are activated.

²⁷M. Marezio, P.D. Dernier, D.B. McWhan, and S. Kachi, *J. Solid State Chem.* **11**, 301 (1974).

²⁸M. Marezio, D.B. McWhan, P.D. Dernier, and J.P. Remeika, *J. Solid State Chem.* **6**, 419 (1973).

²⁹S. Asbrink, *Acta Crystallogr., Sect. B: Struct. Crystallogr. Cryst. Chem.* **36**, 1332 (1980).

³⁰K. Kosuge, *J. Phys. Chem. Solids* **28**, 1617 (1967).

³¹H. Jagodzinski, *Acta Crystallogr.* **7**, 300 (1954).

³²P. Tolédano and V. Dmitriev, *Reconstructive Phase Transitions* (World Scientific, Singapore, 1996).

³³V.P. Dmitriev, S.B. Rochal, Yu.M. Gufan, and P. Tolédano, *Phys.*

Rev. Lett. **60**, 1958 (1988); **62**, 2495 (1989).

³⁴P. Tolédano, G. Krexner, M. Prem, H.-P. Weber, and V.P. Dmitriev, *Phys. Rev. B* **64**, 144104 (2001); O. Blaschko, V. Dmitriev, G. Krexner, and P. Tolédano, *ibid.* **59**, 9095 (1999).